Full-Field Accommodation in Rhesus Monkeys Measured Using Infrared Photorefraction

Lin He, Mark Wendt, and Adrian Glasser

Purpose. Full-field photorefraction was measured during accommodation in anesthetized monkeys to better understand the monkey as a model of human accommodation and how accommodation affects off-axis refraction.

Methods. A photorefraction camera was rotated on a 30-cm-long rod in a horizontal arc, with the eye at the center of curvature of the arc so that the measurement distance remained constant. The resistance of a potentiometer attached to the rotation center of the rod changed proportionally with the rotation angle. Photorefraction and rotation angle were simultaneously measured at 30 Hz. Trial-lens calibrations were performed on-axis and across the full field in each eye. Full-field refraction measurements were compared using on-axis and full-field calibrations. In five iridectomized monkeys (mean age in years ± SD: 12.8 ± 0.9), full-field refraction was measured before and during carbachol iontophoresis stimulated accommodation, a total of seven times (with one repeat each in two monkeys).

Results. Measurements over approximately 20 seconds had <0.1 D of variance and an angular resolution of 0.1°, from at least −30° to 30°. Photorefraction calibrations performed over the full field had a maximum variation in the calibration slopes within one eye of 90%. Applying full-field calibrations versus on-axis calibrations resulted in a decrease in the maximum SDs of the calculated refractions from 1.99 to 0.89 D for relative peripheral refractive error and from 4.68 to 1.99 D for relative accommodation.

Conclusions. By applying full-field calibrations, relative accommodation in pharmacologically stimulated monkeys was found to be similar to that reported with voluntary accommodation in humans. (*Invest Ophthalmol Vis Sci.* 2012;53:215–223) DOI: 10.1167/iovs.11-8324

There is growing interest in understanding peripheral refraction as a cue for myopia progression. Studies on peripheral refraction date back to the 1930s, when refraction was measured up to an eccentricity of 60° temporally or nasally in human subjects.[1–3] Peripheral refraction was later measured in a much larger population that considered the role of peripheral refractive error in the development of central myopia.[4–6] The results showed a relatively higher risk for young emmetropic pilots with peripheral hyperopia to develop central myopia than those with peripheral myopia.[6] Subsequently, many studies have investigated the question of whether peripheral refraction can affect the development of myopia in humans[7–12] and in animals.[13,14] In rhesus monkeys, if the fovea is ablated and the periphery is form deprived, peripheral refractive error can still affect emmetropization.[13,14] These findings suggested peripheral refraction in both humans and rhesus monkeys may be related to progression of myopia and imply that factors affecting peripheral refraction may have an impact on myopia development.

When the eye accommodates for foveal tasks, peripheral refraction must also change. Accommodation has been linked to the progression of myopia.[15–17] However, it is not clear exactly how accommodation affects peripheral refraction or whether the central and peripheral refractive changes are similar. Several studies[18–25] have investigated the relationship between accommodation and peripheral refraction in humans (Table 1). If there is a significant difference between the central and peripheral refraction during accommodation, this means that a large amount of defocus may occur in the periphery, even though accommodation reduces central defocus. Large defocus in the periphery might then induce foveal myopia.[13] This could be regarded as a peripheral mechanism of development of refractive error. If there is little difference between the central and peripheral refraction during accommodation, accommodation is neither an exaggerating nor a damping factor for peripheral mechanism in developing central refractive errors.

To understand how accommodation affects peripheral refraction, full-field measurement with a high angular resolution can be helpful. Most studies measured peripheral refraction at about every 10° (see Table 1). One study[23] achieved an angular resolution of 0.4° using photorefraction. In myopic eyes some retinal regions of higher refractive variations have been identified compared with emmetropic eyes.[26] The more irregular peripheral refraction was suggested as an early indicator of myopia progression. Full-field refraction measurement with high angular resolution can provide more detailed information across the retinal field and therefore a better understanding of peripheral refraction.

Rhesus monkeys have been used to study myopia[27] and accommodation,[28] but no prior studies have demonstrated how peripheral refraction changes during accommodation in rhesus monkeys and whether it is similar to humans. Understanding this is of significance to demonstrate if rhesus monkeys are a good animal model for human accommodation and myopia studies[13] from the aspect of peripheral refraction. In this study, a photorefraction system was developed to measure full-field refraction in rhesus monkeys to understand the relationship between accommodation and peripheral refraction. A comparison of results from the present study to the human studies listed in Table 1 was used to evaluate if drug-stimulated accommodative changes in peripheral refraction in rhesus monkeys are similar to those with voluntary accommodation in humans.

From the College of Optometry, University of Houston, Houston, Texas.

Supported in part by National Eye Institute/National Institutes of Health CORE Grant P30 EY07551.

Presented in part at the annual meeting of the Association for Research in Vision and Ophthalmology, Fort Lauderdale, Florida, May 2011.

Submitted for publication July 30, 2011; revised October 12 and November 16, 2011; accepted November 18, 2011.

Disclosure: **L. He**, None; **M. Wendt**, None; **A. Glasser**, None

Corresponding author: Adrian Glasser, College of Optometry, University of Houston, 4901 Calhoun Road, Houston, TX 77204; aglasser@optometry.uh.edu.

Table 1. Studies on the Relationship between Accommodation and Peripheral Refraction

Method	Study	Eccentricity Range	Step	Relative Accommodation
Autorefraction	Smith, Millodot, and McBrein, 1988[22]	−60° to 60° (H and V)	10°	EM: + (H); uni (V)
	Walker and Mutti, 2002[24]	−30° to 30° (H)	30°	BO: +
	Whatham, Zimmermann, Martinez, et al., 2002[25]	−40° to 40° (H)	10°, 20°	MY: −
	Davies and Mallen, 2009[19]	−30° to 30° (H)	10°	BO: uni
Shack–Hartmann aberrometry	Calver, Radhakrishnan, Osuobenil, et al., 2007[18]	−30° to 30° (H)	10°	BO: +
	Mathur, Atchison, and Charman, 2009[21]	−21° to 21° (H)	7°	EM: uni (H); + (V)
		−20° to 20° (V)	5°	
	Lundström, Mira-Agudelo, and Artal, 2009[20]	−40° to 40° (H)	10°	EM: − (H); uni (V)
		−20° to 20° (V)		MY: uni (H); + (V)
Photorefraction	Tabernero and Schaeffel, 2009[23]	−45° to 45° (H)	0.4°	EM: uni

"H" and "V" represent the horizontal and the vertical meridians; "+," "−," and "uni" represent hyperopic, myopic, and uniform changes in relative peripheral refractive error during accommodation. "EM," "MY," and "BO" indicate that subjects included were emmetropes, myopes, or both.

Methods

Full-Field Photorefraction System

The photorefraction system was composed of a monochrome digital charge-coupled device camera (DMK 21BU04; The Imaging Source, LLC, Charlotte, NC) with a frame rate up to 60 Hz, a manual focus macro lens (MicroNIKKOR 55 mm f/2.8; Nikon Inc., Melville, NY), and a custom-built USB-powered infrared (IR) light-emitting diode (LED) photorefractor. The camera was attached to a ball joint on top of a vertical pole. The pole was attached to a 30-cm-long horizontal rod that was fixed on one end at a pivot point below the monkey head. The monkey was positioned so the first Purkinje image of the photorefractor LEDs was in focus. The rod was manually rotated in a horizontal arc with the first Purkinje image at the center of curvature of the arc. A potentiometer with a DC power supply was attached to the pivot point of the rod so the potentiometer resistance changed proportionally with the rotation angle (Fig. 1). The analog output from the potentiometer enabled dynamic recording of the angle of rotation through a 240-Hz A/D converter (DI-158U; DATAQ Instruments, Inc., Akron, OH).

Calibration between the eccentricity of the camera and the voltage across the potentiometer was performed with a linear regression at the beginning of each experiment. Figure 2 shows an example of a calibration function. The r^2 values for all angle calibration functions were >0.99.

A real-time software application (Matlab; The MathWorks, Inc., Natick, MA) was developed to acquire and analyze photorefraction images and simultaneously record the angular eccentricity at 30 Hz. The implementation of photorefraction (in Matlab) is similar to that described previously and measures refraction and accommodation only in the vertical meridian.[29,30] Astigmatism was not able to be measured. Because the eyes were iridectomized and no clear pupillary margin exists, pupil diameter was not measured. The first Purkinje image was tracked and a predetermined fixed 40% proportion of the entrance pupil aperture was used for photorefraction analysis. Full-field and on-axis trial-lens photorefraction calibrations were performed in every experiment to convert photorefraction slope to refraction. Lenses of powers ranging from −2 to 10 D in 2-D steps were mounted in this order in front of the eye attached to the photorefractor rod. The trial lenses were aligned with the optical axis of the camera and were rotated in an arc centered on the Purkinje image together with the photorefractor camera during the full-field calibration procedure. The camera recorded at 30 Hz and the full-field sweep (−30° to +30°) of the camera and the trial lens took approximately 20 seconds. This resulted in approximately 600 calibration measurements, with each trial lens at an angular resolution of 0.1°. Although this results in abundant calibration data at an unnecessarily high angular resolution, the system and software design made this the simplest and most rapid method for collecting and applying the full-field calibrations. Reducing the camera and software acquisition frequency would have reduced the data file sizes, but would have conferred no other advantages. The calibration data were saved to a file and later automatically applied through software control.

Animal Preparation

All experiments conformed to the ARVO Statement for the Use of Animals in Vision Research and were performed in accordance with institutionally approved animal protocols. Experiments were performed on the left eyes of five rhesus monkeys (*Macaca mulatta*), a total of seven times (with one repeat each in two monkeys). The monkeys ranged in age from 11.3 to 13.6 years (mean age in years ± SD: 12.8 ± 0.9). These monkeys were previously used in myopia

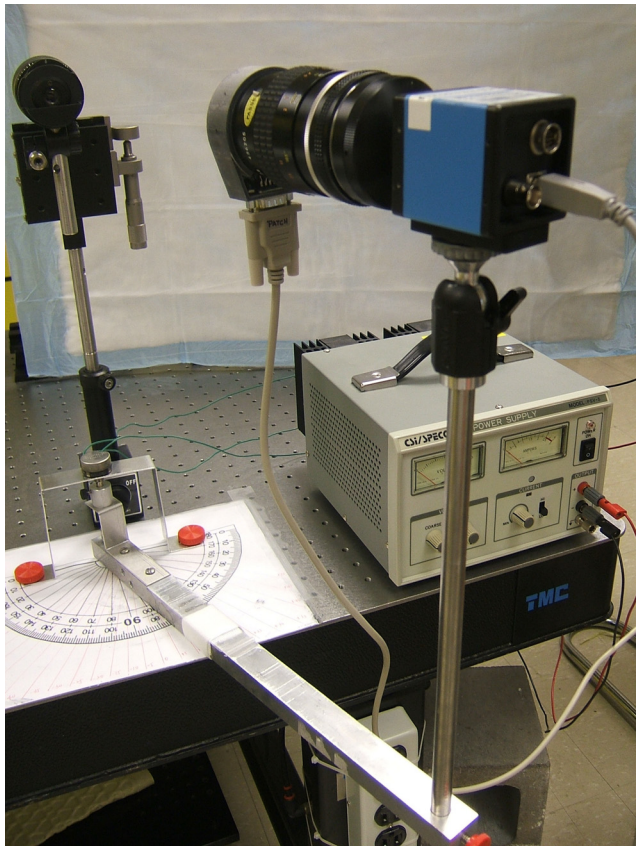

Figure 1. The full-field photorefraction system was tested by measuring full-field refraction on a model eye. The system consists of a photorefractor and camera mounted on a vertical pole, a power supply, a potentiometer, and a horizontal rotating rod.

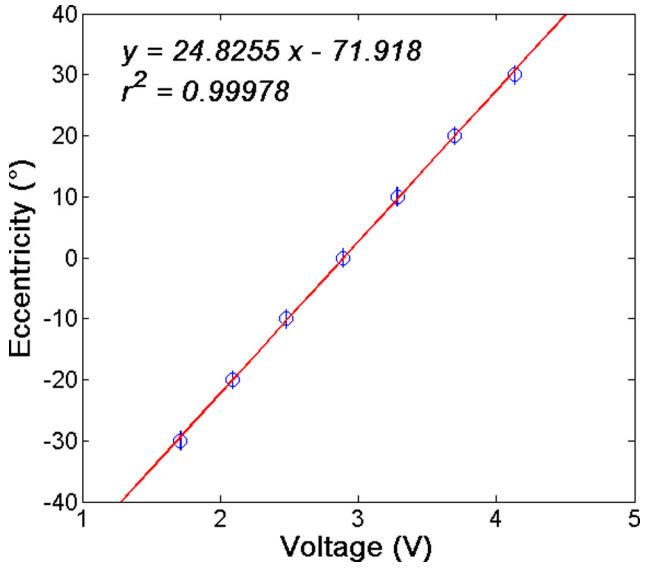

FIGURE 2. An example of an angular calibration performed by positioning the horizontal rod at several known eccentricities and measuring the corresponding voltage. Such calibrations were performed at the start of each experiment and were used to convert recorded voltage to eccentricity.

studies several years ago. The eyes were iridectomized for prior accommodation experiments[31] so the strong pupil constrictions that would otherwise occur with drug stimulation did not prevent the experiments from being performed. For each experiment, monkeys were sedated first with intramuscular 15 mg/kg ketamine (Phoenix Pharmaceutical, St. Joseph, MO) and then anesthetized with constant intravenous infusion of 0.5 mg/kg/min propofol (Abbott Laboratories, North Chicago, IL). Vital signs including temperature, pulse rate, and SpO_2 were monitored and recorded. A heating pad was wrapped around the monkeys to maintain body temperature around 37°C. Throughout the experiment, the monkey head was held upright and facing forward in a head holder. The eyelids were held open with a speculum and a rigid PMMA contact lens was placed on the cornea to prevent corneal dehydration throughout the experiment. The contact lenses were −3-, 0-, or +3-D lenses custom-designed to approximately fit the corneal curvature of the monkey eyes with an optic zone diameter of 11 mm and a total diameter of 12 mm. The selection of lens power was based on the baseline refraction of each individual monkey to shift the refractions toward the middle of the working range of the photorefractor and to slightly offset the high myopic refractions that occur with accommodation. Radii of base curvatures ranged from 6.25 to 6.75 mm and were chosen to best fit the individual monkeys. Contact lenses are generally stable on the eyes, although some contact lens movement could occur if the eyes were to move. When needed, sutures were placed through the lateral and medial rectus muscles to minimize wandering eye movements that sometimes occur under propofol anesthesia. Alignment of the photorefractor with the eye of the anesthetized monkey was determined at the start of each experiment by adjusting the height and angle of the photorefractor camera using the vertical pole and the ball joint, respectively, and by moving the monkey to get the first Purkinje image as centered within the iridectomized eye as possible and in focus for all camera angles.

Stimulation and Measurement of Accommodation

Accommodation was stimulated using carbachol iontophoresis[32,33]; 40% carbachol in agar gel was applied iontophoretically for 8 seconds each to the nasal and temporal regions of the cornea. The eye was immediately irrigated with saline and the contact lens placed on the cornea. Photorefraction measurements commenced and after maximum accommodation was reached, carbachol iontophoresis was given for the second time for 4 seconds to nasal and temporal cornea to ensure that maximum accommodation was achieved. Full-field refraction was measured before and starting at every 2 minutes after carbachol iontophoresis stimulated accommodation until no further change in accommodation occurred. For each full-field measurement, the photorefractor was manually rotated in an arc centered and focused on the first Purkinje image of the contact lens from −30° to 30° over a period of approximately 20 to 30 seconds. The virtual first Purkinje image is located approximately 3 mm behind the first surface of the contact lens, depending on the radius of curvature of the contact lens.

Photorefraction Calibration

Conversion from the photorefraction-measured slope to refraction[29] was calibrated in two ways. First, photorefraction slopes measured at all eccentricities were converted to refraction with the on-axis (0°) trial-lens calibration function. Second, the photorefraction slope at each eccentricity at 0.1° intervals was converted by applying calibration functions determined at each of the corresponding 0.1° eccentricities. The trial-lens calibration slopes, which were acquired at intervals of 0.1° for seven trial lenses of different powers, were fit with linear functions and were applied to the full-field measurements, automatically through software control. On-axis calibration functions were generated using the 0° calibration data. Refractions determined using the on-axis calibration function and full-field calibration functions were compared.

Data Analysis

Relative peripheral refractive error (RPRE), without and with contact lenses, and relative accommodation were calculated from the measurements from each eye. For each full-field refraction measurement, RPRE was defined as peripheral refraction at all eccentricities relative to the on-axis (0°) refraction. Relative accommodation was defined as accommodative response at all eccentricities relative to the accommodative response on axis (at 0°). At each eccentricity at intervals of 0.1°, RPRE and relative accommodation from all the monkeys were averaged and SDs were calculated. Comparing the 600 SDs of RPRE or relative accommodation measurements at all eccentricities, the maximal SD for a specific eccentricity was used as an indicator of how much RPRE and relative accommodation varied between monkeys and over the visual field.

RESULTS

To test the reproducibility of the system, the full-field refraction in one monkey eye was measured four times during a 2-minute interval in the unaccommodated state (Fig. 3). The sharp myopic shift (approximately 4° in Fig. 3) was caused by measuring over the optic nerve head during the scan. Since much stronger reflection of the IR light from the optic nerve head usually saturates the photorefraction image, these myopic regions around the optic nerve head were regarded as artifacts and were excluded in later analysis. For example, when means and SDs were calculated across the full field, the roughly 10° around the peak of the artifact was excluded, wherever that artifact occurred for that particular eye. This artifact due to the optic nerve head was not present in every eye because the line of sight of the eye of each anesthetized monkey varied slightly relative to the photorefractor due to the position of the head in the head holder and the position of the eye in the orbit. The repeatability of the system was defined, from these four repeated scans on the same eye. The SD at 0.1° intervals was determined from the four repeated refraction measurements and the average SD from all eccentricities was found to be 0.09 D. Other characteristics of the current system will be compared with prior full-field refraction measurement systems[23,34] in the Discussion section.

An example of the full-field calibration (including the on-axis calibration) from one eye showing the linear regression lines fit to the calibration functions, relating the measured

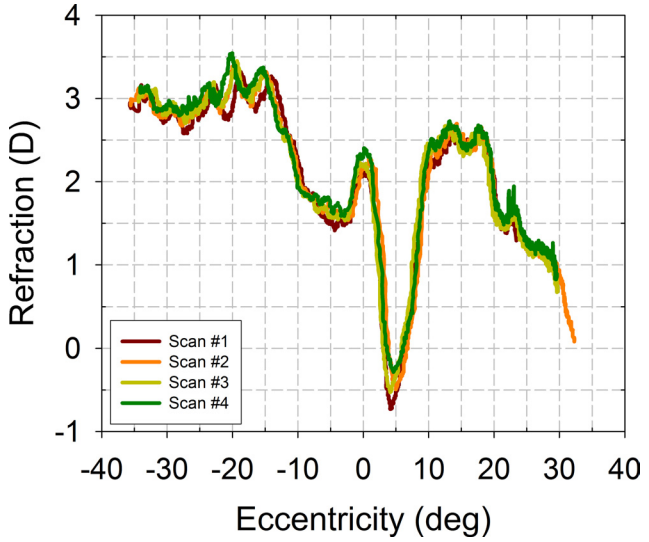

FIGURE 3. Four repeated refraction measurements as a function of eccentricity from the same unaccommodated monkey eye. The myopic trough at approximately 5° is caused by the optic nerve head.

photorefraction slopes to the powers of the trial lenses held in front of the eye at every 0.1° interval, is shown in Figure 4.

To determine how similar the on-axis calibration functions were to the full-field calibration functions, all the calibration functions except over the region corresponding to the optic nerve head (+10° to +20°) were plotted. Figure 5 shows two typical examples (the least variation and the most variation). The large variations in slopes and intercepts that can occur (Figs. 5C, 5D) means that if only the on-axis calibration is used to convert photorefraction slopes to refraction values at all eccentricities in this eye, large variations in refraction would occur relative to the results from applying the full-field calibrations. The means and SDs of slopes (b_1) and the range of slopes (b_1), intercepts (b_0), and r^2 values from the calibration functions from all experiments are shown in Table 2.

Figure 6 shows an example of full-field refraction changes from before to after carbachol-stimulated accommodation. Each 30-Hz full-field refraction measurement (Fig. 6A, individual blue traces) took approximately 20 seconds to complete and 30 individual full-field refraction measurements were performed at approximately 2-minute intervals over a period of 60 minutes. The surface fit (Fig. 6B) illustrates how the full-field refraction map changes with accommodation. The photorefraction measurements shown in this experiment were calibrated to refraction using full-field calibrations.

Figures 7A–D show RPRE without and with a contact lens on the cornea and relative accommodation (Figs. 7E, 7F) as a function of full-field eccentricities. Figures 7A, 7C, and 7E show the results after applying on-axis calibration functions, whereas Figures 7B, 7D, and 7F show the results after applying full-field calibration functions. The variation of RPRE and relative accommodation across the full field is shown in gray as the SD at all the measured eccentricities. Applying the full-field calibrations reduced the maximum SDs for RPRE without contact lenses from 3.29 to 2.87 D, reduced RPRE with contact lenses from 1.99 to 0.89 D, and reduced relative accommodation with contact lenses from 4.68 to 1.99 D. Based on the results from Figure 7F, there is, in general, a slightly larger accommodative response in the periphery relative to the on-axis response during carbachol iontophoresis stimulated accommodation in rhesus monkeys.

DISCUSSION

Measurement of Full-Field Refraction

The system used in the present study allowed a constant distance between the camera and the measured eye over the full field and permitted full-field photorefraction calibrations to be performed by rotating the trial lens in front of the eye coaxially with the photorefraction camera. Photorefraction, orthogonal,[35] isotropic,[36] and eccentric,[37,38] has been applied to measure refraction for several decades. Orthogonal photorefraction, the forerunner to photorefraction, allowed binocular refraction measurement at a distance. Isotropic photorefraction allowed determination of the sign of defocus. Eccentric, video-based photorefraction[39,40] allows dynamic measurements of a wider range of refractive errors. These advantages enable eccentric photorefraction to be more widely used in studying accommodation, myopia, strabismus, and amblyopia in humans[41,42] and animals.[29,43,44] The ability of photorefraction to do dynamic recordings makes it possible to measure the full-field refraction and accommodation with a high angular resolution in <30 seconds.[23,26] Prior studies used a fast scanning mirror that allowed the full-field refraction measurement to be performed in 4 seconds without moving the camera. However, since the distance from the camera to the scanning mirror and then from the mirror to the eye varied by approximately 10 to 20 cm over the full field, the first Purkinje image in the photorefraction image can be out of focus at some points in the scan, especially if a large camera aperture is used. In the present study the photorefractor was rotated, which ensured the image was in focus all the time and allowed full-field trial-lens calibrations to be performed by moving the trial lens with the camera coaxially.

The need to apply full-field calibration was investigated in the present study. To convert slope to real refraction using an

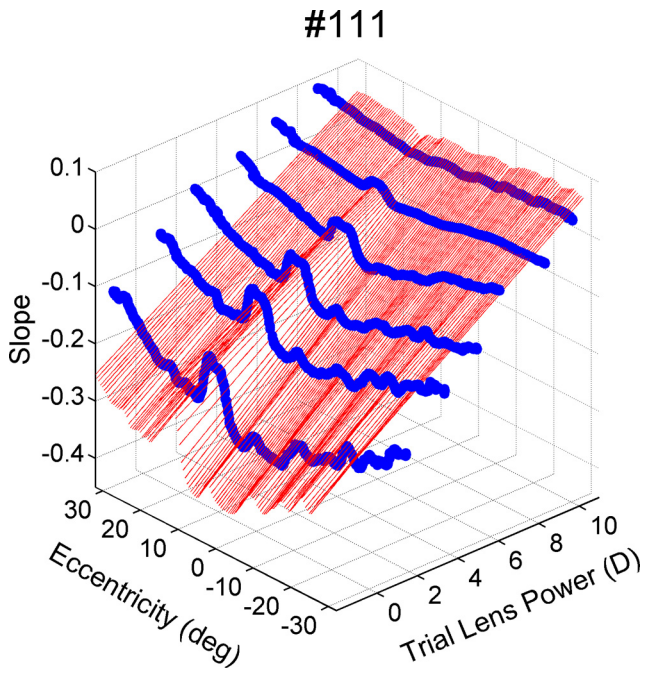

FIGURE 4. Full-field (−30° to +30°) photorefraction trial lens (0 D to +10 D) calibrations in one eye. The *blue traces* are slopes as a function of trial-lens power and eccentricity. Linear regression lines (*red lines*) are shown only at 0.5° intervals to reduce the density of the lines so they can be distinguished. At between +5° and +15° (nasal retina) on the graph, large deviations of the regression lines were caused by increased reflectance from the optic nerve head during photorefraction.

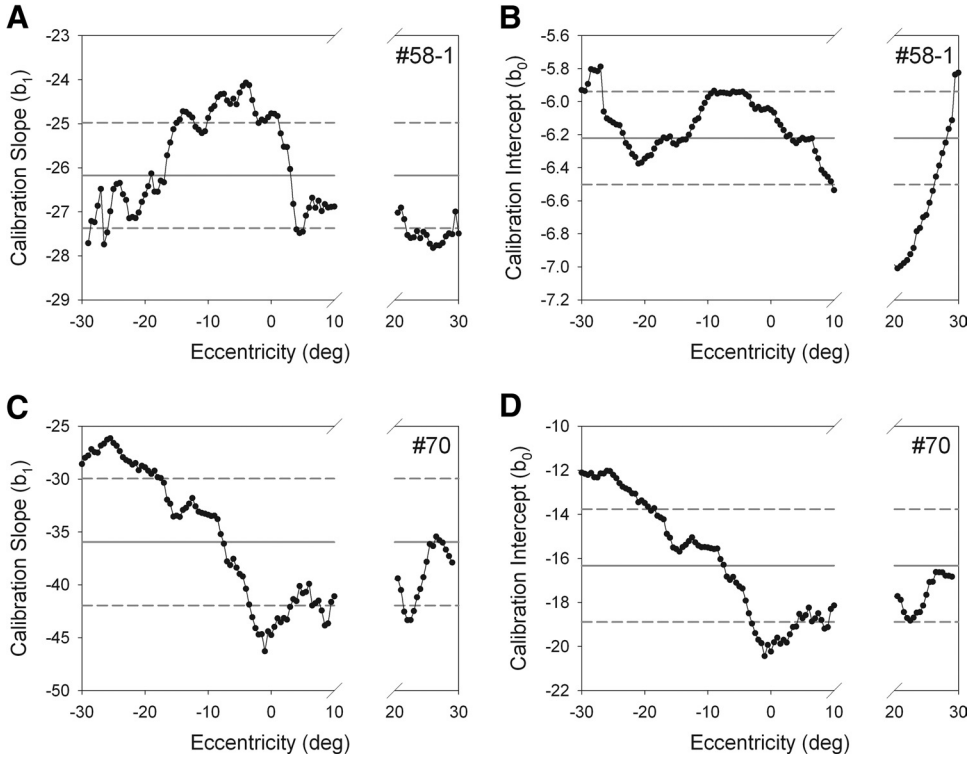

FIGURE 5. Slopes (b_1) and intercepts (b_0) of full-field linear calibrations (except over the optic nerve head) as a function of eccentricity in two eyes at 0.5° intervals. The graphs are plotted to different *y*-axis scales. Monkey 58 shows relatively little difference in slopes (**A**) and intercepts (**B**), whereas monkey 70 shows a larger range of slopes (**C**) and intercepts (**D**).

on-axis calibration, only one on-axis calibration function is necessary. However, for the full-field photorefraction measurement, it was possible to generate different calibration functions at different eccentricities with an angular resolution as small as 0.1°. Prior studies on human subjects suggested off-axis calibration functions were not significantly different from the on-axis calibration function, which justified their application of a single calibration function to all eccentricities.[23] Although in some cases, the on-axis photorefraction calibration functions can be similar to off-axis calibration functions (Figs. 5A, 5B), Figures 5C and 5D suggest that applying only the on-axis calibration gives different results compared with applying the full-field calibrations. Applying only an on-axis calibration function might overestimate the relative accommodation (Fig. 7). Applying the full-field calibrations with photorefraction provides more accurate results. The large interindividual variation in the mean slopes of the calibration functions with relatively small SDs demonstrates that the calibration functions are dependent on the individual eyes. This interindividual variability is likely due to monkeys having individual differences in fundus reflectivity as has previously been demonstrated in humans.[45] Even in the same monkey, for example in monkey 58 (Table 2), calibration functions can differ due to different camera settings or differences in eye alignment.

Effect of Rigid Contact Lenses on Peripheral Refraction

A rigid contact lens was placed on the cornea of each eye to prevent corneal dehydration and to ensure maintenance of good optical quality. In studies of peripheral refraction in humans, myopic subjects wore soft contact lenses,[19,24,25] trial lenses,[18] or spectacles[20] for correcting their central refractive errors. One study[19] shows no significant effect on peripheral refraction from soft contact lenses and another study[20] found little change in peripheral refraction with and without spectacles if the spectacles remained perpendicular to the measurement axis. When peripheral refraction without and with soft or rigid contact lenses was compared in human subjects,[46] rigid contact lenses shifted the field curvature by twice as much as soft contact lenses. Results portrayed in the present study showed very different peripheral refraction without and with rigid contact lenses (Figs. 7A–D). Although the contact lenses used are standard lenses and are not designed to custom fit each eye, interestingly, the rigid contact lenses tended to reduce the peripheral refractions (Figs. 7B, 7D). This is consistent with the prior study,[46] which reported that eyes having rigid contact lenses had most emmetropic peripheral refraction compared with the naked eyes or the eyes with soft

TABLE 2. Means and SDs of Photorefraction Calibration Slopes (b_1) and the Range of Slopes (b_1), Intercepts (b_0), and r^2 Values for Full-Field Trial Lens Calibrations in All Eyes

Monkey	b_1 mean	b_1 SD	b_1 min	b_1 max	b_0 min	b_0 max	r^2 min	r^2 max
54	−53.19	2.82	−49.02	−60.00	−4.86	−5.43	0.912	0.953
58–1	−26.11	1.20	−24.00	−27.83	−5.82	−7.02	0.902	0.990
70	−35.31	5.90	−26.09	−46.36	−12.01	−20.50	0.588	0.951
58–2	−14.36	0.96	−13.15	−16.35	−5.20	−6.47	0.940	0.959
65–1	−43.37	1.90	−40.57	−48.99	−8.98	−11.76	0.846	0.953
111	−37.90	2.97	−33.49	−45.30	−7.30	−8.79	0.857	0.965
65–2	−40.62	3.24	−35.23	−45.85	−8.85	−11.80	0.804	0.919

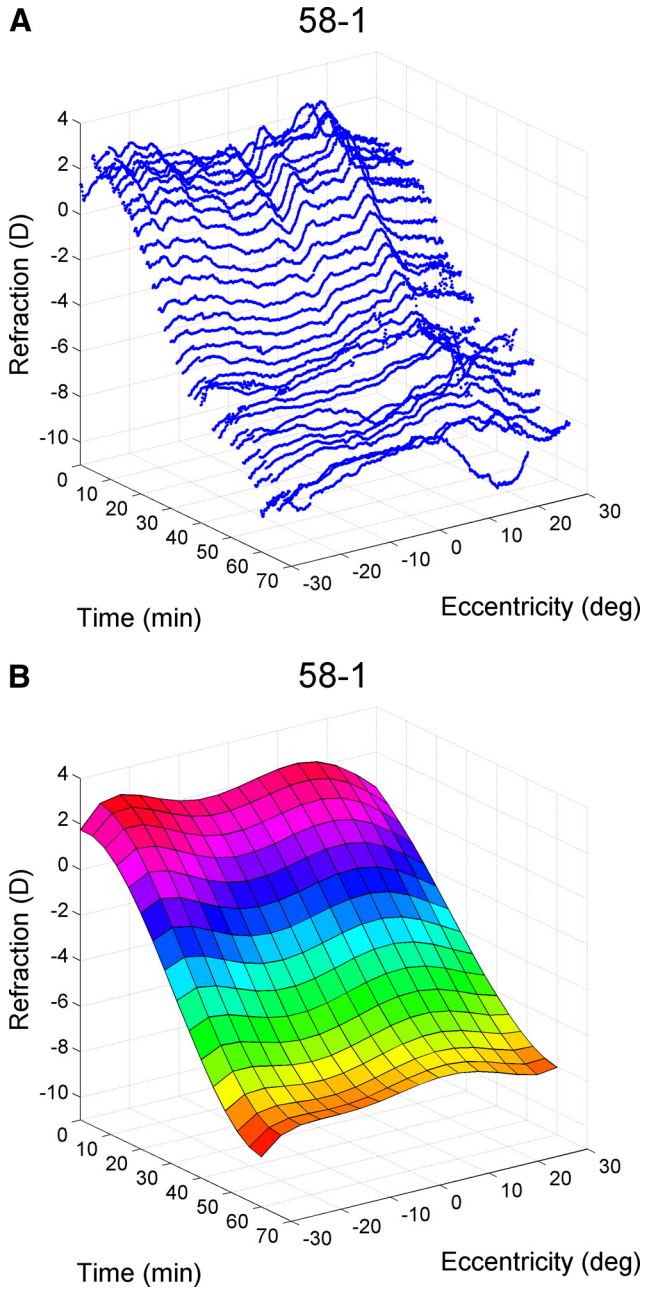

FIGURE 6. **(A)** Full-field refraction change after carbachol iontophoresis stimulated accommodation with time in one monkey. The full-field calibration is applied to this graph. **(B)** The surface fit is a third-order polynomial in time axis and a fifth-order polynomial in eccentricity axis. The flat shape along the eccentricity axis suggests that full-field refraction changed uniformly during accommodation.

contact lenses. The spherical rigid contact lens reduces the asphericity of the cornea. The prior study showed that peripheral astigmatism increased with eccentricity,[46] although in the present study, refraction measured with the custom photorefractor was always only in the vertical/sagittal meridian and so astigmatism could not be measured.

Changes of Full-Field Refraction with Accommodation

With the rigid contact lenses on the eye and when applying the full-field calibration functions, the full-field refraction changes relatively uniformly during accommodation. Three of the five eyes in the present study were myopic because the monkeys were used in prior myopia studies. The relative accommodation is slightly less at the periphery than on-axis (Fig. 7F). Whether the previous manipulations of these monkey eyes had any effect on the relative accommodation is uncertain, but the current result is consistent with what has been found in most myopic human eyes.[18–24] One study[25] found a relative myopic shift in the far peripheral visual field (40°) with accommodation in myopes. Although these studies included subjects with varied refractive errors, used different instruments and accommodative stimuli, and measured peripheral refraction in different ways, relatively uniform full-field refraction changes with accommodation have been found in almost all studies (Table 1). This indicates that accommodation has a similar impact on refraction change over the full field.

In this study, accommodation was stimulated with carbachol iontophoresis in anesthetized rhesus monkeys. Pharmacologically induced accommodation has shown larger response amplitudes than centrally stimulated accommodation in monkeys, likely due to muscarinic cholinergic agonists causing a maximal contraction of all ciliary muscle fibers, which may not occur with central stimulation.[33,47] Goniovideography provides evidence to support this hypothesis by showing larger centripetal movements of ciliary process and crystalline lens edge with pharmacologic versus central stimulation.[48] Therefore, muscarinic cholinergic agonists such as carbachol and pilocarpine can be regarded as a supramaximal accommodative stimulus. In addition, topical pilocarpine can produce different ocular biometric changes from voluntary accommodation in humans. Significant anterior shifts of the crystalline lens and artificial intraocular lens[49,50] occur during pilocarpine-induced accommodation but not during voluntary accommodation. This anterior shift of the lens has also been observed during carbachol-induced accommodation[33] but not during Edinger–Westphal (EW)-stimulated accommodation in monkeys.[33,51] Whether this different accommodative response for pharmacologic stimulation will cause different refraction change over the full field is not known. Prior studies[18–24] show uniform full-field refraction changes during voluntary accommodation in humans. The results in the present study also demonstrate relatively uniform full-field refraction change in carbachol-induced accommodation in monkeys. This suggests the different ocular biometric changes between voluntary accommodation in humans and carbachol-induced accommodation in anesthetized monkeys do not result in different full-field refraction changes. Although drug-stimulated accommodation was used here in rhesus monkeys, the similarity in these results with those found in conscious humans adds further validation for the use of rhesus monkeys as a model to study human accommodation and the progression of myopia.

Limitations

Unlike in human studies, the monkeys in the present study were anesthetized and could not fixate. The alignment of the photorefractor with the eye was mainly judged by aligning the first Purkinje image with the center of the iridectomized eye exit pupil. The precise determination of the azimuth and elevation of the 0° visual axis in this study is therefore subjective and likely to differ between different monkeys. This can be observed through the existence and the location of the photorefraction artifact from the optic nerve head in Figure 7. Not all the monkeys show the optic nerve head artifact, which suggests the measurement axes for different monkeys were vertically offset. The location of the optic nerve head varies among the monkeys, which suggests horizontal alignment was slightly

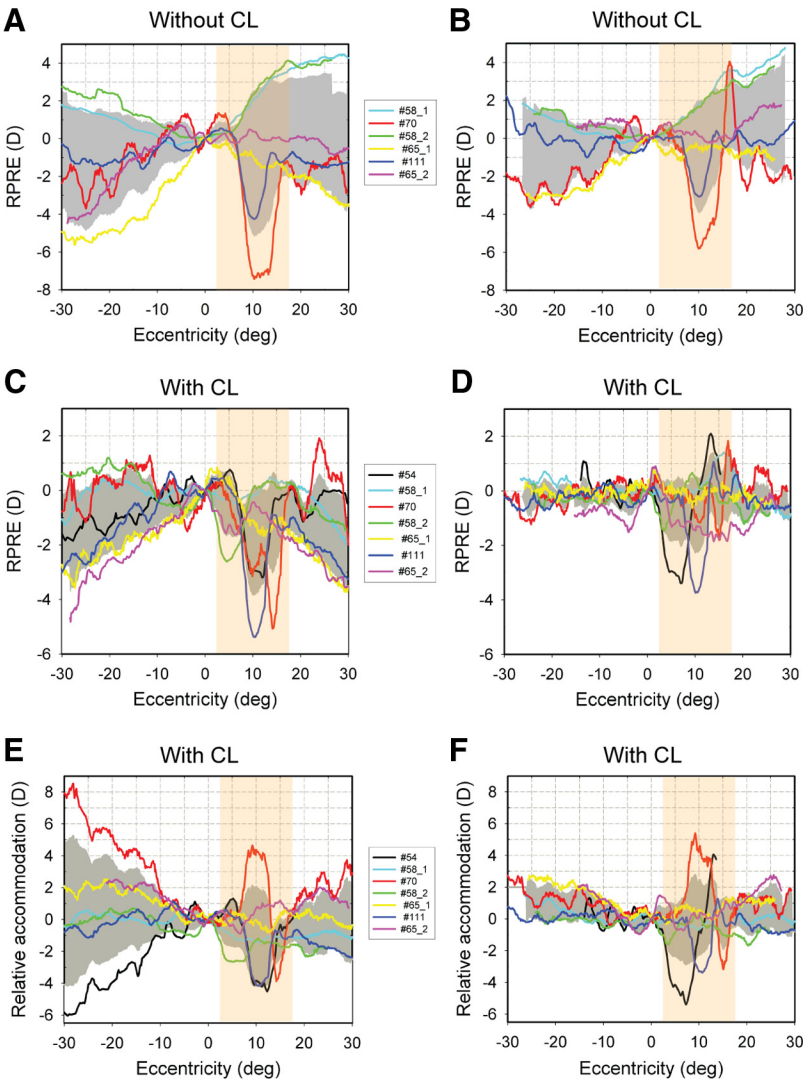

FIGURE 7. RPRE without and with contact lens, and relative accommodation as a function of eccentricity for all experiments. (**A**, **C**, **E**) Used on-axis (0°) photorefraction calibration. (**B**, **D**, **F**) Used full-field calibrations. *Dark gray areas* represent the mean ± 1SD of all data shown. *Light orange areas* represent the optic nerve head artifacts (+2.5° to +17.5°). The averaged relative accommodation over the full field in (**F**) is relatively flat, demonstrating that full-field refraction changed relatively uniformly during accommodation.

different. If eye movements occur during the calibration procedure, changes in the optic nerve head artifact can affect the calibration functions.

The monkey eyes were all iridectomized. The iridectomy allows the lens edge and the ciliary processes to be observed to study the accommodative mechanism.[48,52] Moreover, the iridectomy prevents marked pupil constriction that would be induced by carbachol and allows performing photorefraction in a large and constant-sized optical zone.[29,53] Surgical iridectomy has been reported to cause a reduction of maximal carbachol-induced accommodative amplitude, but not in EW-stimulated accommodation.[54] It is suggested that drug-induced iris constriction further pulls the ciliary body and decreases the ciliary ring diameter. Even so, the fundamental accommodative mechanism is unaffected by the iridectomy.[28,54] The iridectomy also means that the alignment of the first Purkinje image with the center of the exit pupil of the iridectomized eye might be different from the center of the exit pupil of the natural pupil with an intact iris. This could also result in differences in eye alignment between different studies. The absence of the iris and a distinct pupil margin also mean that it is not possible to measure and calculate the Hirschberg ratio in these eyes as has previously been done with photorefraction in human eyes.[55]

Nasotemporal refractive asymmetries were reported in prior studies,[20,26,56,57] whereas the present study in monkeys did not show obvious asymmetries. Two groups[26,58] inferred the asymmetry in human eyes was mainly caused by angle λ/κ (angle κ was redefined as the same angle between the line of sight and pupillary axis as angle λ by Le Grand[59]). In other words, it was suggested that if the pupillary axis instead of the line of sight was regarded as on-axis (0°), the peripheral refraction would be symmetric. Although in the on-axis condition the first Purkinje image of the monkeys was initially aligned with the center of the exit pupil of the iridectomized eye instead of the center of exit pupil of the natural pupil, the more symmetric full-field refractions shown in this study (Fig. 7) suggests that this alignment axis is similar to the pupillary axis.

Compared with the prior systems used to measure full-field refraction,[23,34] the system described in the present study has not been motorized. Motorization would speed up the measurements and may be helpful in large population-based studies. Both of the previously described motorized systems[23,34] and the system used in the present study are capable of only horizontal full-field refraction measurements. So far, off-axis measurement in the vertical meridian has been achieved by presenting targets only at different vertical loci to shift the fixation of the subject. This would mean the resolution in the vertical meridian relies on the precision of fixation of the testing subject.

Conclusions

Dynamic, full-field refraction during pharmacologic stimulated accommodation has been performed in anesthetized monkeys. Variability of peripheral refraction during accommodation is reduced substantially by applying full-field calibrations. Relative accommodation with pharmacologic stimulation in monkeys is similar to that in human voluntary accommodation reported previously.[18–24]

Acknowledgments

The authors thank Chris Kuether and Charles Neff for technical assistance.

References

1. Ferree CE, Rand G, Hardy C. Refraction for the peripheral field of vision. *Arch Ophthalmol.* 1931;5:717–731.
2. Ferree CE, Rand G, Hardy C. Refractive asymmetry in the temporal and nasal halves of the visual field. *Am J Ophthalmol.* 1932;15: 513–522.
3. Ferree CE, Rand G. Interpretation of refractive conditions in the peripheral field of vision. *Arch Ophthalmol.* 1933;9:925–938.
4. Rempt F, Hoogerheide J, Hoogenboom WP. Influence of correction of peripheral refractive errors on peripheral static vision. *Ophthalmologica.* 1976;173:128–135.
5. Rempt F, Hoogerheide J, Hoogenboom WP. Peripheral retinoscopy and the skiagram. *Ophthalmologica.* 1971;162:1–10.
6. Hoogerheide J, Rempt F, Hoogenboom WP. Acquired myopia in young pilots. *Ophthalmologica.* 1971;163:209–215.
7. Atchison DA, Pritchard N, Schmid KL, Scott DH, Jones CE, Pope JM. Shape of the retinal surface in emmetropia and myopia. *Invest Ophthalmol Vis Sci.* 2005;46:2698–2707.
8. Logan NS, Gilmartin B, Wildsoet CF, Dunne MC. Posterior retinal contour in adult human anisomyopia. *Invest Ophthalmol Vis Sci.* 2004;45:2152–2162.
9. Millodot M. Effect of ametropia on peripheral refraction. *Am J Optom Physiol Opt.* 1981;58:691–695.
10. Mutti DO, Hayes JR, Mitchell GL, et al. Refractive error, axial length, and relative peripheral refractive error before and after the onset of myopia. *Invest Ophthalmol Vis Sci.* 2007;48:2510–2519.
11. Seidemann A, Schaeffel F, Guirao A, Lopez-Gil N, Artal P. Peripheral refractive errors in myopic, emmetropic, and hyperopic young subjects. *J Opt Soc Am A Opt Image Sci Vis.* 2002;19:2363–2373.
12. Mutti DO, Sinnott LT, Mitchell GL, et al. Relative peripheral refractive error and the risk of onset and progression of myopia in children. *Invest Ophthalmol Vis Sci.* 2011;52:199–205.
13. Smith EL 3rd, Kee CS, Ramamirtham R, Qiao-Grider Y, Hung LF. Peripheral vision can influence eye growth and refractive development in infant monkeys. *Invest Ophthalmol Vis Sci.* 2005;46: 3965–3972.
14. Smith EL 3rd, Ramamirtham R, Qiao-Grider Y, et al. Effects of foveal ablation on emmetropization and form-deprivation myopia. *Invest Ophthalmol Vis Sci.* 2007;48:3914–3922.
15. Abbott ML, Schmid KL, Strang NC. Differences in the accommodation stimulus response curves of adult myopes and emmetropes. *Ophthalmic Physiol Opt.* 1998;18:13–20.
16. Gwiazda J, Bauer J, Thorn F, Held R. A dynamic relationship between myopia and blur-driven accommodation in school-aged children. *Vision Res.* 1995;35:1299–1304.
17. Gwiazda J, Thorn F, Bauer J, Held R. Myopic children show insufficient accommodative response to blur. *Invest Ophthalmol Vis Sci.* 1993;34:690–694.
18. Calver R, Radhakrishnan H, Osuobeni E, O'Leary D. Peripheral refraction for distance and near vision in emmetropes and myopes. *Ophthalmic Physiol Opt.* 2007;27:584–593.
19. Davies LN, Mallen EA. Influence of accommodation and refractive status on the peripheral refractive profile. *Br J Ophthalmol.* 2009; 93:1186–1190.
20. Lundström L, Mira-Agudelo A, Artal P. Peripheral optical errors and their change with accommodation differ between emmetropic and myopic eyes. *J Vis.* 2009;9:Art. 17.
21. Mathur A, Atchison DA, Charman WN. Effect of accommodation on peripheral ocular aberrations. *J Vis.* 2009;9:Art. 20.
22. Smith G, Millodot M, McBrien NA. The effect of accommodation on oblique astigmatism and field curvature of the human eye. *Clin Exp Optom.* 1988;71:119–125.
23. Tabernero J, Schaeffel F. Fast scanning photoretinoscope for measuring peripheral refraction as a function of accommodation. *J Opt Soc Am A Opt Image Sci Vis.* 2009;26:2206–2210.
24. Walker TW, Mutti DO. The effect of accommodation on ocular shape. *Optom Vis Sci.* 2002;79:424–430.
25. Whatham A, Zimmermann F, Martinez A, et al. Influence of accommodation on off-axis refractive errors in myopic eyes. *J Vis.* 2009; 9:1–13.
26. Tabernero J, Schaeffel F. More irregular eye shape in low myopia than in emmetropia. *Invest Ophthalmol Vis Sci.* 2009;50:4516–4522.
27. Hung LF, Crawford ML, Smith EL. Spectacle lenses alter eye growth and the refractive status of young monkeys. *Nat Med.* 1995;1:761–765.
28. Glasser A, Kaufman PL. The mechanism of accommodation in primates. *Ophthalmology.* 1999;106:863–872.
29. Vilupuru AS, Glasser A. Dynamic accommodation in rhesus monkeys. *Vision Res.* 2002;42:125–141.
30. Wendt M, Glasser A. Topical and intravenous pilocarpine stimulated accommodation in anesthetized rhesus monkeys. *Exp Eye Res.* 2010;90:605–616.
31. Kaufman PL, Lütjen-Drecoll E. Total iridectomy in the primate in vivo: surgical technique and postoperative anatomy. *Invest Ophthalmol Vis Sci.* 1975;14:766–771.
32. Koretz JF, Bertasso AM, Neider MW, True-Gabelt B, Kaufman PL. Slit-lamp studies of the rhesus monkey eye. II. Changes in crystalline lens shape, thickness and position during accommodation and aging. *Exp Eye Res.* 1987;45:317–326.
33. Ostrin LA, Glasser A. Comparisons between pharmacologically and Edinger-Westphal–stimulated accommodation in rhesus monkeys. *Invest Ophthalmol Vis Sci.* 2005;46:609–617.
34. Jaeken B, Lundstrom L, Artal P. Fast scanning peripheral wavefront sensor for the human eye. *Opt Express.* 2011;19:7903–7913.
35. Howland HC, Howland B. Photorefraction: a technique for study of refractive state at a distance. *J Opt Soc Am.* 1974;64:240–249.
36. Howland HC, Braddick O, Atkinson J, Howland B. Optics of photorefraction: orthogonal and isotropic methods. *J Opt Soc Am.* 1983;73:1701–1708.
37. Kaakinen K, Tommila V. A clinical study on the detection of strabismus, anisometropia or ametropia of children by simultaneous photography of the corneal and the fundus reflexes. *Acta Ophthalmol (Copenh).* 1979;57:600–611.
38. Schaeffel F, Farkas L, Howland HC. Infrared photoretinoscope. *Appl Opt.* 1987;26:1505–1509.
39. Bobier WR, Braddick OJ. Eccentric photorefraction: optical analysis and empirical measures. *Am J Optom Physiol Opt.* 1985;62: 614–620.
40. Howland HC. Photorefraction and videorefraction of eyes: past, present, and future. *J Opt Soc Am.* 1993:83:142–145.
41. Choi M, Weiss S, Schaeffel F, et al. Laboratory, clinical, and kindergarten test of a new eccentric infrared photorefractor (PowerRefractor). *Optom Vis Sci.* 2000;77:537–548.
42. Kasthurirangan S, Glasser A. Age related changes in accommodative dynamics in humans. *Vision Res.* 2006;46:1507–1519.
43. Schaeffel F, Burkhardt E, Howland HC, Williams RW. Measurement of refractive state and deprivation myopia in two strains of mice. *Optom Vis Sci.* 2004;81:99–110.
44. Bossong H, Swann M, Glasser A, Das VE. Applicability of infrared photorefraction for measurement of accommodation in awake-behaving normal and strabismic monkeys. *Invest Ophthalmol Vis Sci.* 2009;50:966–973.
45. Schaeffel F, Wilhelm H, Zrenner E. Inter-individual variability in the dynamics of natural accommodation in humans: relation to age and refractive errors. *J Physiol.* 1993;461:301–320.

46. Shen J, Clark CA, Soni PS, Thibos LN. Peripheral refraction with and without contact lens correction. *Optom Vis Sci.* 2010;87:642–655.
47. Crawford K, Terasawa E, Kaufman PL. Reproducible stimulation of ciliary muscle contraction in the cynomolgus monkey via a permanent indwelling midbrain electrode. *Brain Res.* 1989;503:265–272.
48. Ostrin LA, Glasser A. Edinger-Westphal and pharmacologically stimulated accommodative refractive changes and lens and ciliary process movements in rhesus monkeys. *Exp Eye Res.* 2007;84:302–313.
49. Koeppl C, Findl O, Kriechbaum K, Drexler W. Comparison of pilocarpine-induced and stimulus-driven accommodation in phakic eyes. *Exp Eye Res.* 2005;80:795–800.
50. Kriechbaum K, Findl O, Koeppl C, Menapace R, Drexler W. Stimulus-driven versus pilocarpine-induced biometric changes in pseudophakic eyes. *Ophthalmology.* 2005;112:453–459.
51. Vilupuru AS, Glasser A. The relationship between refractive and biometric changes during Edinger-Westphal stimulated accommodation in rhesus monkeys. *Exp Eye Res.* 2005;80:349–360.
52. Croft MA, Kaufman PL, Crawford KS, Neider MW, Glasser A, Bito LZ. Accommodation dynamics in aging rhesus monkeys. *Am J Physiol Regul Integr Comp Physiol.* 1998;275:R1885–R1897.
53. Baumeister M, Wendt M, Glasser A. Edinger-Westphal stimulated accommodative dynamics in anesthetized, middle-aged rhesus monkeys. *Exp Eye Res.* 2008;86:25–33.
54. Crawford KS, Kaufman PL, Bito LZ. The role of the iris in accommodation of rhesus monkeys. *Invest Ophthalmol Vis Sci.* 1990;31:2185–2190.
55. Schaeffel F. Kappa and Hirschberg ratio measured with an automated video gaze tracker. *Optom Vis Sci.* 2002;79:329–334.
56. Atchison DA, Pritchard N, Schmid KL. Peripheral refraction along the horizontal and vertical visual fields in myopia. *Vision Res.* 2006;46:1450–1458.
57. Dunne MC, Misson GP, White EK, Barnes DA. Peripheral astigmatic asymmetry and angle alpha. *Ophthalmic Physiol Opt.* 1993;13:303–305.
58. Berntsen DA, Mutti DO, Zadnik K. Validation of aberrometry-based relative peripheral refraction measurements. *Ophthalmic Physiol Opt.* 2008;28:83–90.
59. Le Grand Y. In: El Hage SG, translator. *Physiological Optics.* London: Springer-Verlag; 1980.